Journal of The Electrochemical Society, **151** (6) C399-C404 (2004)
0013-4651/2004/151(6)/C399/6/$7.00 © The Electrochemical Society, Inc.

Reaction of Si with HCl to Form Chlorosilanes

Time Dependent Nature and Reaction Model

Suguru Noda,[z] Katsuaki Tanabe, Takashi Yahiro, Toshio Osawa, and Hiroshi Komiyama

Department of Chemical System Engineering, School of Engineering, The University of Tokyo, Tokyo 113-8656, Japan

We propose a chemical vapor deposition (CVD) process with closed gas recycling for making low-cost, crystalline silicon thin films for solar cells, which connects chlorosilane synthesis from Si and HCl with Si thin-film growth by CVD from chlorosilanes. In this work we studied the formation of chlorosilanes by the reaction of Si with HCl at temperatures ranging from 623 to 723 K. The reaction rate is time dependent, and many pores are formed on the surface of particles after reaction. These pores are active sites for chemical reactions, and the reaction rates increase with increasing pore area. The rate can be correlated with the conversion ratio of Si, and the temporal evolution of the reaction rate can be explained by a reaction model called the shrinking-core model with growing pores. By using this model, we estimated the reaction rates per unit area of activated surfaces and converted them into a rate equation that can be used for the reactor design. The incubation time of the reaction can be shortened by pretreating the Si particles in a fluidized bed, which probably creates defects in the native oxide layers on the particles, which in turn become reactive sites.
 [DOI: 10.1149/1.1737386]

Manuscript submitted April 26, 2003; revised manuscript received January 2, 2004. Available electronically May 4, 2004.

Crystalline Si solar cells are commonly used because of their high efficiency, stability, and relatively low production costs. For such solar cells to be widely used, however, continued production cost reductions are still needed. Because Si substrates account for about half of the module costs, new low-cost production processes are needed for forming the Si photovoltaic layer. Si substrates are currently made by slicing Si ingots, each of which constitutes about 1000 μm thickness of the ingot, including the thickness required for cutting. Using such a thick layer of silicon is one source of the relatively high costs of these solar cells. Substituting Si substrates with Si thin films is a promising approach for cost reduction and several processes so-called layer transfer processes have been developed to produce either monocrystalline or large-grained polycrystalline Si thin films.[1] Because the higher deposition temperature of active Si layers tends to produce higher open-circuit cell voltage,[1] Si chemical vapor deposition (Si-CVD) from chlorosilanes at high temperatures is suitable for photovoltaic layer formation.

In CVD thin film growth, to maintain high film uniformity, the reactant conversion ratio is usually kept low and the residual gases are discarded because they may contain particulates and contaminants. This low conversion efficiency of high-purity Si results in relatively high production costs. To overcome this problem, we propose a CVD process with closed gas recycling, in which the outlet gases of the CVD reactor are recycled to the reactor to synthesize chlorosilanes from metallurgical-grade Si (MG-Si) particles and HCl gas (Fig. 1).[2] The reactions for this process can be expressed as

$$\text{MG-Si} + x\text{HCl} \rightarrow \text{SiH}_{4-x}\text{Cl}_x + (x-2)\text{H}_2 \quad [1]$$

$$\text{SiH}_{4-x}\text{Cl}_x + (x-2)\text{H}_2 \rightarrow \text{SOG-Si} + x\text{HCl} \quad [2]$$

which are reversible, and the direction can be controlled mainly by temperature, as shown in Fig. 2. In this process, MG-Si powder is converted into solar-grade Si (SOG-Si) thin films, with high Si-reactant-to-film conversion efficiency and minimum consumption of H and Cl.

This reaction system is similar to the Siemens process, which is one of the standard processes for synthesizing high-purity Si from MG-Si. In the Siemens process, however, chlorosilanes are decomposed near equilibrium conditions to thicken polycrystalline Si seed rods, which are then used to form Si ingots. By changing the form of Si products from rods to thin films, we can obtain areas of Si photovoltaic layers that are more than an order of magnitude larger than that available by using substrates cut from ingots. To design a CVD process with closed gas recycling, kinetic information on the reactants is needed because the reactions are controlled kinetically especially in thin-film growth in CVD reactors, and also because it is needed to properly model the complicated interaction between the two reactors of chlorosilane production and Si-CVD. Because the Siemens process is well-established and is controlled thermodynamically rather than kinetically, little information is available in the open literature on the kinetics of this reaction system. Therefore, we investigated the reaction kinetics both for chlorosilane synthesis and for Si deposition. We report the former reaction in this paper.

Most studies related to Reaction 1 have been oriented towards Si-wafer cleaning processes that typically operate at temperatures, $T > 1300$ K,[3-11] and few studies have been made at temperatures near 800 K,[12] where Reaction 1 is thermodynamically favored, as shown in Fig. 2. The main products of Reaction 1 are trichlorosilane ($SiHCl_3$) and silicontetrachloride ($SiCl_4$),[13,14] and copper is useful as a catalyst[3,15,16] to drive Reaction 1. But this information is insufficient for designing the reaction system.

In this work, we experimentally investigated the reaction of HCl with Si particles to form chlorosilanes by using a fluidized-bed reactor at temperatures ranging from 623 to 723 K. A model called the shrinking-core model with growing core was also developed to explain the time-dependent nature of this reaction and also to extract the reaction rate of active Si surfaces.

Experimental

The fluidized-bed reactor was made of a silica glass tube with an outer diameter of 24 mm, an inner diameter of 22 mm, and a height

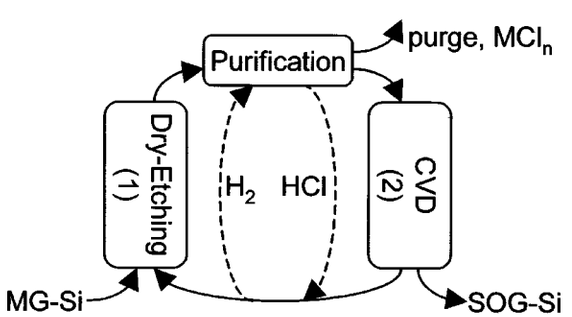

Figure 1. Conceptual view of the CVD process with closed gas recycling.

[z] E-mail: noda@chemsys.t.u-tokyo.ac.jp

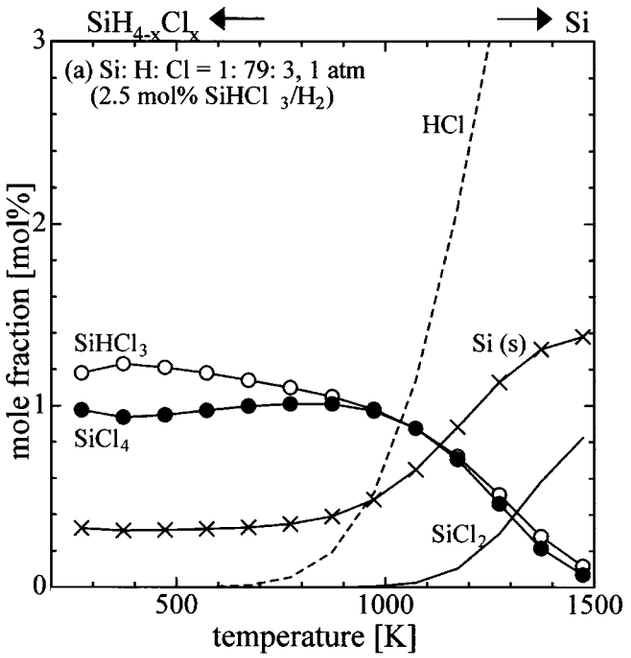

Figure 2. Thermodynamic equilibrium composition of an Si/H/Cl system *vs.* temperature.

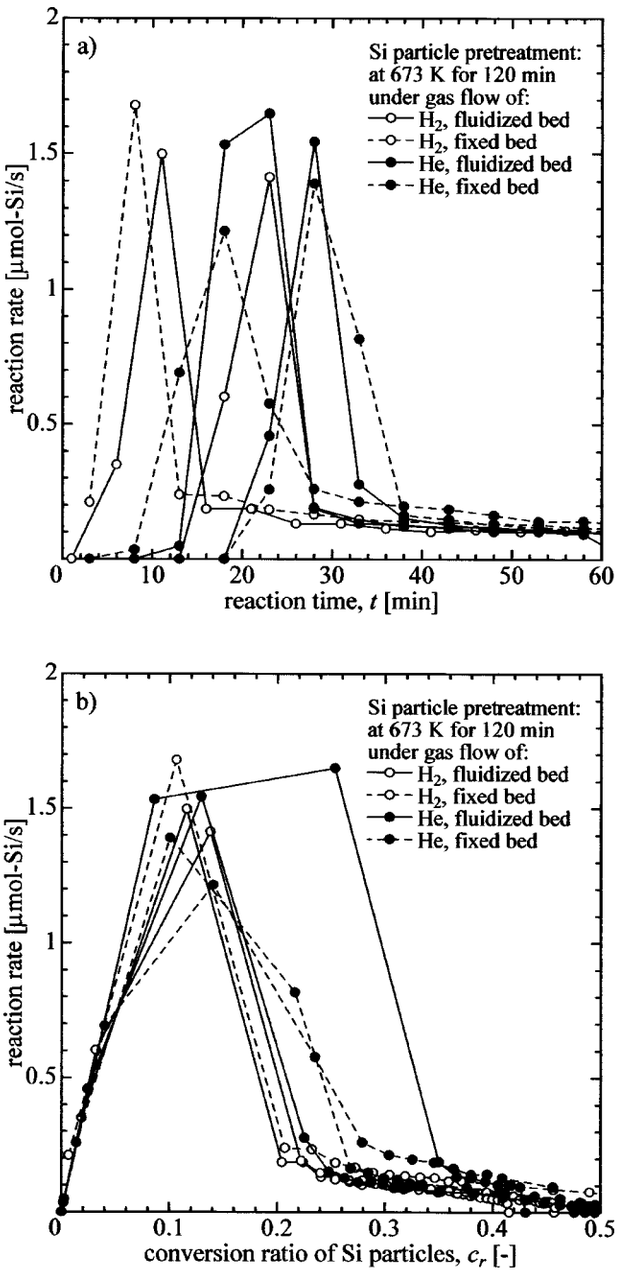

Figure 3. Reaction rate of Si particles at HCl concentration, C_{HCl} = 3.3 vol %, and T = 673 K. The reaction rate was time dependent and did not correlate well with reaction time, t (a), but correlated well with Si conversion ratio, c_r (b).

of 250 mm. The temperature was controlled by using an external cylindrical heater 200 mm high. We filled the reactor with 0.08 g of Si particles and 19.92 g of silica particles, both of which had sieve diameters between 90 and 150 μm. We investigated the reaction of both MG-Si (98 wt %) and high-purity Si (99.9 wt %) particles, and the reaction rates were almost the same for these two types of Si particles. Most of the results reported here are for MG-Si particles, however, for the experiment examining the effect of pretreatment, we used high-purity Si particles (Fig. 3). Silica was used as a fluidization medium. The porosity of the fluidized bed was 0.56. To dry the particles and to remove organic impurities from the surface of the particles, either H_2 or He was run through the reactor for 0 to 150 min at T = 673 or 773 K and a gas flow rate, Q = 100 or 300 sccm. The particles were in the fixed-bed condition (*i.e.*, nonfluidized) for Q = 100 sccm, whereas they were in the fluidized-bed condition for Q = 300 sccm. After this pretreatment, the gas was switched to a HCl/H_2 mixed gas, and the reaction was started. The reaction conditions were pressure, $P = 9.0 \times 10^4$ Pa, T = 623, 673, or 723 K, Q = 300 sccm, and the concentration of HCl, C_{HCl} = 1.0, 3.3, or 10 vol %. The fraction of each gas was measured at the exit of the reactor by using gas chromatography, and the reaction rate was calculated as the conversion rate of Si to chlorosilanes. To satisfy the differential reactor assumption, the reaction conditions were set to keep the conversion ratio of HCl low.

Because the reaction rate was time-dependent, we analyzed Si particles after the reaction. In these experiments, 5.0 g of Si particles were fed into the reactor without silica particles, and their conversion ratio was calculated from the ratio of the amount of the chlorosilanes produced to the amount of the Si particles initially fed. Optical microscopy (OM) was used for measuring the size distribution of the particles, and scanning electron microscopy (SEM) was used for determining the surface morphology of the particles. The surface area of the unreacted and reacted Si particles were measured by using Brunauer-Emmett-Teller (BET) N_2 adsorption.

In addition, Si wafers with and without native oxide layers were used in the reaction to investigate the influence of the native oxide layer on the reaction between HCl and Si. Si wafers without native oxide layers were prepared by pretreating the Si wafers with 5 vol % hydrofluoric acid (HF_{aq}). The wafers were placed in a silica-glass tube-reactor and then reacted with a HCl/H_2 mixed gas for 5 h. The operating conditions were $P = 9.0 \times 10^4$ Pa, T = 673 K, Q = 300 sccm, and C_{HCl} = 3.3 vol %. The surface of these wafers was also observed by OM after the reaction.

Results and Discussion

Time-dependent reaction rate and pretreatment of Si particles.—The main reaction products were $SiHCl_3$ and $SiCl_4$, and $SiCl_4$ concentrations were less than 1 vol % of the $SiHCl_3$ concentrations. Typical reaction rates are shown in Fig. 3a, which indicate that the reaction rates were time dependent and that their repeatabil-

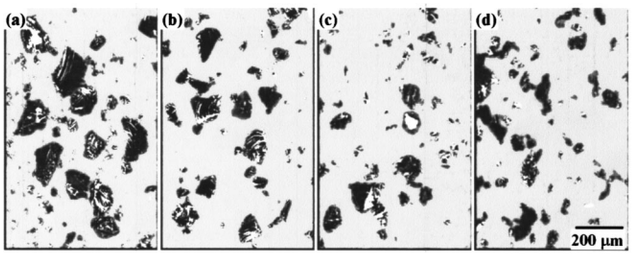

Figure 4. OM images of Si particles for Si conversion ratios, c_r = (a) 0 (before reaction), (b) 0.1, (c) 0.3, and (d) 0.75.

ity was poor between runs made using the same operating conditions. However, once the reaction began, the time dependence of the reaction-rate was repeatable. Figure 3b shows the reaction rates *vs.* conversion ratio of Si particles, c_r. c_r was calculated from the amount of the chlorosilane produced and the amount of the Si particles initially fed. Because some particles were blown out of the reactor during the reaction by becoming small enough to be suspended in the flowing gas, c_r did not increase to 1. Figure 3b clearly shows that the reaction rate is well correlated with c_r.

When the particles were fluidized with H_2 for 120 min at T = 773 K before the reaction, incubation time became negligible, and the time evolution of reaction rates became repeatable as shown in Fig. 9. We selected this procedure as the standard pretreatment condition of Si particles for the following experiments.

Structural change of Si particles during reaction.—Typical OM images are shown in Fig. 4, and the measured size distributions are shown in Fig. 5. They indicate that the particle size decreases as the reaction proceeds. Many particles below the lower cut point of the sieve diameter (90 μm) existed in the nonreacted Si particles, but their influence on the reaction was negligible because their total surface area was insignificant compared to the total surface area of the particles. Most of these particles disappeared in the regime c_r < 0.1, which indicates that they reacted and disappeared early in the reaction process.

Figure 6a shows a typical SEM image of Si particles, which indicates that the reaction proceeds locally to form many pores. Because these pores were observed on the surfaces of both MG-Si and high-purity Si particles after reaction, contamination should not be the cause for the formation of these pores. Another possibility causing this uneven surface morphology is in the native oxide layers on the surface of Si particles. To determine the influence of native oxide layers on the reaction with HCl, we made experiments using two kinds of Si wafers instead of Si particles. One wafer had its native oxide layer removed by etching it with HF_{aq} before reaction, and the other wafer was used without this etching pretreatment. As a result, as shown in Fig. 6b, the reaction occurred over the entire surface of the HF_{aq}-etched wafer, but as shown in Fig. 6c, etch-pits appeared on the unetched wafer. The production of such etch-pits results from surface reactions at a limited number of active points on the surface where there are probably breaks in the oxide layer. This

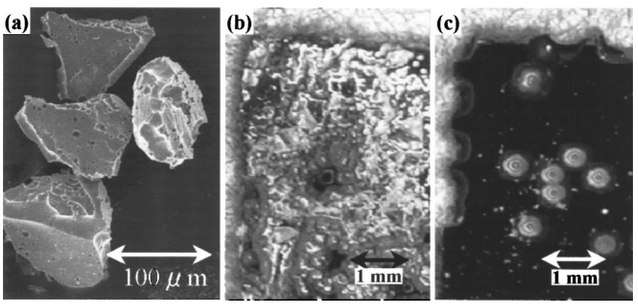

Figure 6. Images of Si surfaces after reaction. (a) SEM image of particles for Si conversion ratio, c_r = 0.1, (b) OM images of Si wafers with (b) and without (c) native oxide layers after reaction at HCl concentration, C_{HCl} = 3.3 vol %, and T = 673 K for 5 h.

implies that native oxide layers prevent Si particles from reacting, except at the breaks in the oxide layers. Apparently chemically reactive areas on the particles are formed during pretreatment in the fluidized state when the native oxide layers are probably eroded by collisions with the particles. Thus, in addition to removing water and organic compounds, the pretreatment enhances the reactivity of the particles.

Figure 7a shows the change of the surface area of Si particles as a function of c_r. The broken line represents the change for a shrinking particle where the reaction occurs over the entire particle surface (shrinking-core model), and the solid line indicates fitting of the measured data with the model we developed, which is explained in the next section. The increase of the surface area at the beginning of the reaction results from the increasing roughness of Si particles (Fig. 6a). A form factor, f, is defined as the ratio of the measured value of the BET surface area to the value calculated by using the shrinking-core model. Initially f = 1, and Fig. 7b shows that f increased with increasing c_r and approached 5.

Reaction model.—We formulated a reaction model to explain the dependence of the surface area and the reaction rate on c_r, by considering the effect of the Si particle shrinking and its surface roughness increasing. Figure 8 shows a schematic of the morphological change of Si particles in our model. In the model we assumed that the Si particles are spheres all of the same size, and that each particle initially has N active points, which are breaks in the native oxide layers from which the reaction starts. We further assumed that the reaction proceeds isotropically at a constant rate R_s (m/s). The new surfaces generated by the reaction become active surfaces and spread. After multiple active surfaces meet and overlap each other, the entire surface becomes activated, and the particles shrink, maintaining a similar shape during shrinkage.

The increase of the etched, outer surface area by the reaction, ΔS_e (m^2), can be represented as

$$\Delta S_e = N \times \Delta[\pi(R_s t)^2] \times \frac{S_0 - S_e}{S_0} \qquad [3]$$

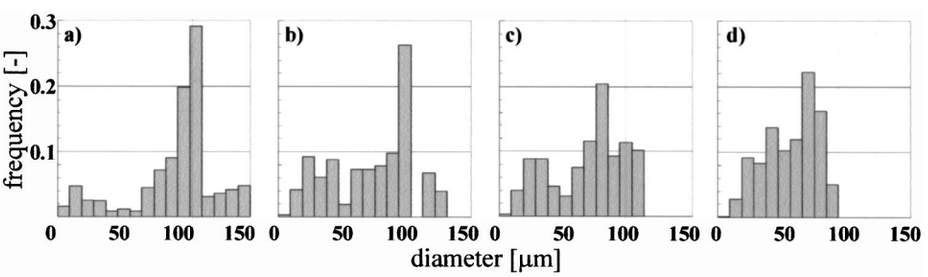

Figure 5. Si particle size distribution for Si conversion ratios, c_r = (a) 0 (before reaction) (500 particles measured), (b) 0.1 (300 particles measured), (c) 0.3 (250 particles measured), and (d) 0.75 (100 particles measured).

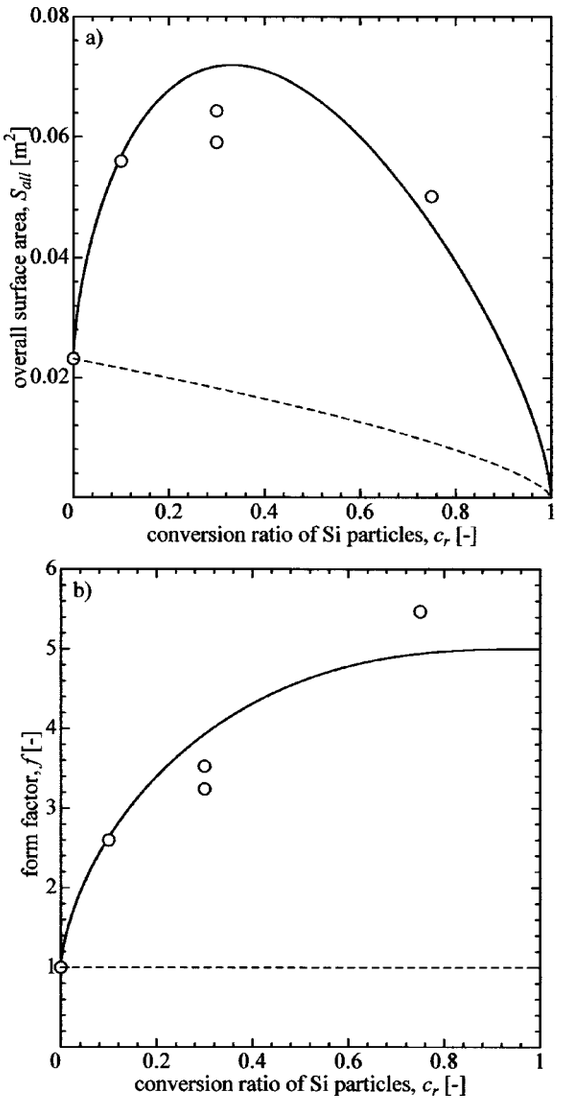

Figure 7. Comparison of experimental and modeling results for the morphological change of Si particles. (a) Surface area experimentally obtained (open circles), that calculated by using the shrinking-core model (broken line), and that calculated by using our model (solid line). (b) Form factor experimentally obtained (open circle), that used in the shrinking-core model (broken line), and that calculated by using our model (solid line).

where t (s) is time, S_0 (m^2) is the initial outer surface area of Si particles before reaction, and $(S_0 - S_e)/S_0$ is the modification coefficient resulting from the overlapping of active surfaces. The time evolution of the area of the inactive surface lost can be expressed as

$$\frac{S_e}{S_0} = 1 - \exp\left(-\frac{\pi N R_s^2}{S_0} t^2\right) \quad [4]$$

We introduce a form factor, f' (dimensionless), which is the ratio of the activated surface area generated to the inactive surface area lost. The time evolution of the active surface area, S_a (m^2), can be expressed as

$$\frac{S_a}{S_0} = f'\left[1 - \exp\left(-\frac{\pi N R_s^2}{S_0} t^2\right)\right] \quad [5]$$

The ratio of the activated surface area to the outer surface area should be expressed with Eq. 5, however, the outer surface itself

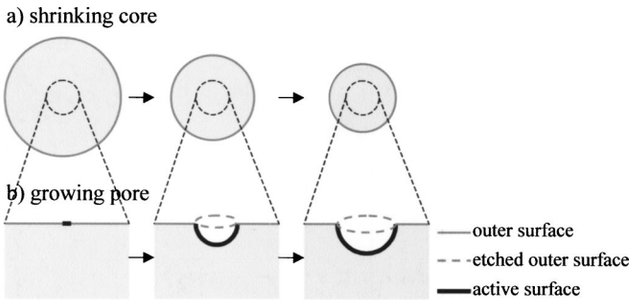

Figure 8. Schematic image of the morphological change of Si particles in our model. (a) Si particle shrinks and (b) pores grow on the surface as the reaction proceeds.

shrinks with time. We incorporated the effect of the change of the outer surface area of Si particles, S (m^2), including both etched and nonetched regions, by substituting S for S_0 in the left side of Eq. 5. By using the shrinking-core model, S can be expressed as

$$S = \left(\frac{V}{V_0}\right)^{2/3} S_0 \quad [6]$$

where V_0 (m^3) and V (m^3) are the volumes of the unreacted and reacted Si particles, respectively. The conversion ratio of Si particles can be expressed as

$$c_r = 1 - \frac{V}{V_0} \quad [7]$$

Because the volume change occurs due to reaction on activated surfaces, it can be expressed as

$$c_r = -\frac{\Delta V}{V_0} = \int \frac{S_a d(R_s t)}{V_0} \quad [8]$$

By substituting Eq. 6 and 7 into Eq. 5, the activated surface area can be expressed as

$$\frac{S_a}{S_0} = f'\left[1 - \exp\left(-\frac{\pi N R_s^2}{S_0} t^2\right)\right](1 - c_r)^{2/3} \quad [9]$$

From Eq. 8 and 9, S_a and c_r can be calculated numerically. The total surface area of Si particles, S_{all}, can be calculated as

$$S_{all} = S - S_e + S_a = S + (f' - 1)S_e \quad [10]$$

and is shown in Fig. 7b. Figure 7 indicates that the changes of both S_{all} and f with c_r is well reproduced by this model. Equation 9 become simple for large t as

$$S_a \to f'(1 - c_r)^{2/3} S_0 \quad (t \to \infty) \quad [11]$$

which is the same as the product of f' times the surface area from the shrinking core model. Thus, the two form factors become the same at high Si conversion ratios, *i.e.*, $f' = f$ for $c_r \to 1$. For a hemispherical active surface, $f' = 2$, however, for reacting Si particles, Fig. 7b indicates that $f' = 5$. In the following discussion, therefore, we use $f' = 5$. Because R_s can be estimated from the measured overall reaction rate and from the BET surface area at high Si conversion ratios, where the entire surface becomes activated, Eq. 9 has only a single fitting parameter, N.

Figure 9 shows measured reaction rates (dots) and the fitted results from our model (lines) *vs.* t for $1.0 \leqslant C_{HCl} \leqslant 10$ vol % and $623 \leqslant T \leqslant 723$ K. For the fitted results, $N = 1000$ and the final conversion ratio of Si particles, $c_{rf} = 0.8$. Note that because of the loss of small particles from the fluidized-bed reactor, $c_{rf} < 1$. The

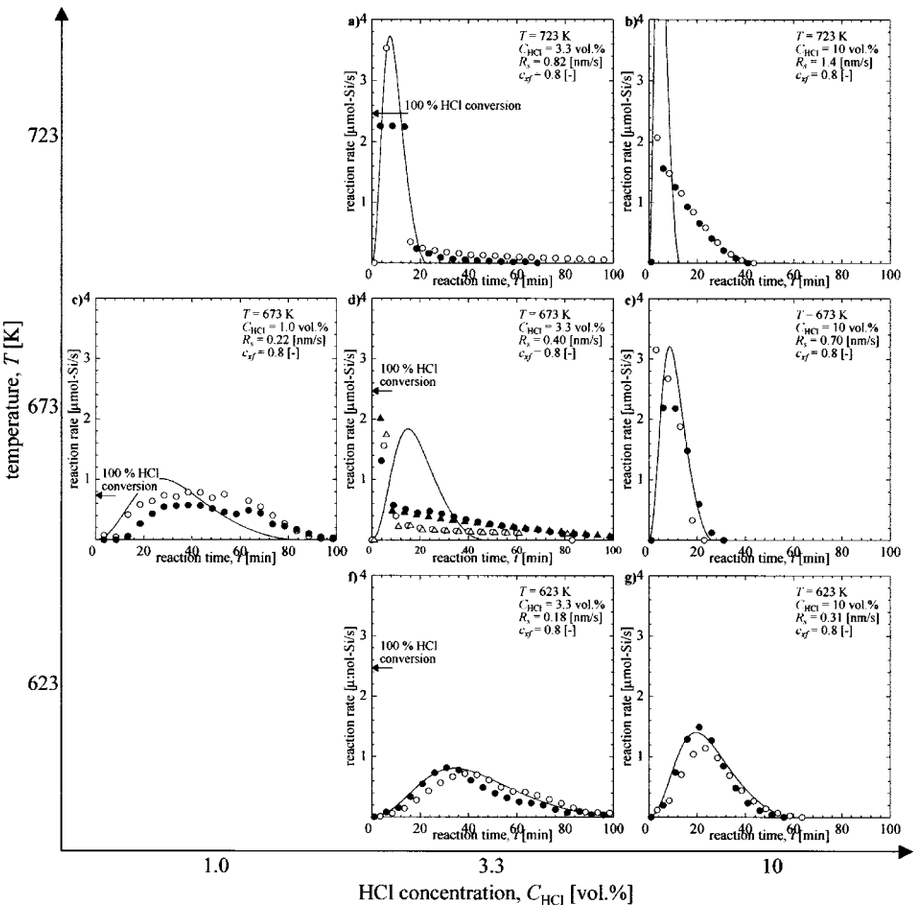

Figure 9. Measured (dots) and calculated (lines) reaction rates of Si particles *vs.* reaction time, *t*, for HCl concentration, C_{HCl} = 1.0 (c), 3.3 (a, d, f), and 10 (b, e, g) vol % at T = 723 (a, b), 673 (c, d, e), and 623 (f, g) K. The symbols show the results of different experimental runs. The experimental results were well represented by our model for (a), (c), (e), (f), and (g), whereas the correlation of the fitted results was poor for (b) and (d).

data in Fig. 9a, c, e, f, and g are well reproduced by the model, except for the short time region of Fig. 9a and c, where the HCl conversion ratio approached 1, and therefore the differential reactor assumption is no longer valid. The reaction rates at the full HCl conversion are 0.74, 2.5, and 7.4 mol-Si/min for C_{HCl} = 1.0, 3.3, and 10 vol %, respectively. For Fig. 9b and d, however, the model results do not agree with the experimental results. The reaction rate began decreasing at relatively low Si conversion ratios. One possible cause of the decreased reaction rate is that either a small amount of oxygen or water impurities reacted with Si surfaces to form oxide layers, inhibiting the reaction of Si surfaces with HCl.

Because the model agreed well with many of the measured data shown in Fig. 9, we conclude that this model reasonably represents the mechanism of the reaction of Si with HCl.

Reaction rate.—We discuss the underlying mechanism for the reaction rate, R_s, in this section. To simplify the discussion, $SiCl_4$ is ignored, whose production rate is less than one-hundredth of $SiHCl_3$. We assumed that the reaction rate of Si, which is the same as the production rate of $SiHCl_3$, is proportional to the area of activated Si surfaces in our model. Actually, our model reproduced the BET surface area as well as the production rate of chlorosilanes by using a constant value for the reaction rate of the activated surfaces, R_s, and thus it is considered that this assumption is reasonable.

As for the dependence of the reaction rate on the HCl concentration, the reaction order appears to be smaller than 1 because the maximum reaction rates in Fig. 9 do not increase linearly with the HCl concentrations. In the model of Fig. 9, we used a reaction rate with a reaction order of 0.5 on HCl concentration and an activation energy of 60 kJ/mol. This reaction rate appears to reproduce the data well. The origin of this reaction rate is discussed next.

The surface area of the 0.08 g of Si particles in Fig. 9 is $3 \times 10^{-4} - 9 \times 10^{-4}$ m^2 for the 0-0.7 conversion ratio, which is estimated from the surface area of the 5 g Si particles in Fig. 7. The feeding rate of reactant HCl is $2 \times 10^{-6} - 2 \times 10^{-5}$ mol/s, and therefore the characteristic time constant for monolayer adsorption can be estimated at around 1 ms. The characteristic time constant of Si consumption is around 10 min, and therefore the adsorption of HCl proves to be in the steady state at each moment of the reaction.

$SiHCl_3$ and H_2 should be the major species desorbing from Si surfaces because no other species like Cl_2 nor $SiCl_2$ are thermodynamically stable under these conditions. If this reaction is of Langmüir-type, it can be expressed as

$$HCl(g) + 2s \rightleftarrows H(s) + Cl(s) \quad [12]$$

$$H(s) + 3Cl(s) + Si(b) \rightleftarrows SiHCl_3(g) + 4s \quad [13]$$

$$2H(s) \rightleftarrows H_2(g) + 2s \quad [14]$$

where (g), (s), and (b) denote the gas-phase, surface, and bulk species, respectively, and s denotes vacant sites of Si surfaces. Under steady-state conditions, these three reactions should be in balance. If Reaction 12 is the rate-determining step, the overall reaction rate should have a reaction order of 1 on HCl concentration, however, the reaction order was around 0.5, and therefore, Reaction 12 proves not to be the rate-determining step. It is reasonable that the desorption reaction, *i.e.*, either Reactions 13 or 14, is the rate-determining step because the reaction order can be less than 1 under desorption-limited conditions. Reaction 14 has been studied extensively.[17-19] Interestingly, H_2 desorption rate at high H coverage is in the first order of H coverage for Si(100) surface,[17,18] whereas it is in the second order for Si(111) surface.[18] From their results, the desorption

rate can be estimated at $5 \times 10^{-4} - 5 \times 10^{-2}$ ML/s at 685-790 K at the full H coverage for both (100) and (111) surfaces. On the other hand, the reaction rate was $0.18 \leqslant R_s \leqslant 1.4$ nm/s, which corresponds to several ML/s. The small desorption rate of H_2 implies that the H_2 desorption is the rate-determining step, however, it is too small to account for the observed reaction rate. One possible reason is the difference in the Si surface structure. The surface was atomically smooth in Ref. 17 and 18, whereas it was rough in this work. As for the activation energy, it was 190-250 kJ/mol for H_2 desorption in Ref. 17 and 18, whereas it was about 60 kJ/mol for R_s in Fig. 9. This large difference in activation energy might also be caused by the difference in the Si surface structure, but we lack information to determine which is the rate-determining step, Reactions 13 or 14. The mechanism of H_2 desorption is still unclear, even for the atomically smooth surfaces of monocrystalline Si.[19]

We summarize the overall production rate of $SiHCl_3$ below. The reaction rate per unit reactor volume, R_{total} (mol/m^3/s), can be expressed as

$$R_{total} = \frac{\rho S_V}{M} R_s \qquad [15]$$

where $\rho = 2.33 \times 10^3$ (kg/m^3) is the density of crystalline Si, S_V (m^2/m^3) is the activated surface area of Si per unit reactor volume, and $M = 28.09 \times 10^{-3}$ (kg/mol) is the atomic weight of Si. The reaction rate used in the model of Fig. 9 was

$$R_s = k c_{HCl}{}^{0.5} \qquad [16]$$

where c_{HCl} (mol/m^3) is the HCl concentration and k (m$^{2.5}$/mol$^{0.5}$/s) is a rate constant expressed as

$$k = 2.5 \times 10^{-5} (\mathrm{m}^{2.5}/\mathrm{mol}^{0.5}/\mathrm{s}) \exp\left[-\frac{60(\mathrm{kJ/mol})}{RT} \right] \qquad [17]$$

where $R = 8.314$ (J/mol/K) is the gas constant. These equations can be used to estimate the production rate of $SiHCl_3$ at $623 \leqslant T \leqslant 723$ K and $0.15 \leqslant c_{HCl} \leqslant 1.8$ mol/m^3.

Conclusions

With the objective of designing a CVD process with closed gas recycling for making low-cost, crystalline silicon thin films for solar cells, we studied the formation of chlorosilanes by the reaction of Si with HCl. The reaction rate was time dependent and did not correlate well with reaction time, but correlated well with the conversion ratio of Si. Many pores were formed on the surface of particles during the reaction, these pores acted as active sites, and the reaction rate increased with increasing pore area. Pretreatment by fluidizing the particles with an H_2 stream for 120 min at $T = 773$ K significantly decreased the incubation time before the reaction started, causing the time profile of the reaction rate to become repeatable. We developed a reaction model called the shrinking-core model with growing pores, and successfully correlated the time-dependent reaction rates with the surface-area change for $623 \leqslant T \leqslant 723$ K and for $1.0 \leqslant C_{HCl} \leqslant 10$ vol%. By using this model, reaction rates per unit area of activated surfaces were estimated and expressed in the form of a rate equation that can be used to design CVD reactors. To realize low-cost production of solar cells, it is important not only to couple the reaction kinetics of chlorosilane synthesis and Si-CVD but also to couple the CVD process with closed gas recycling[2] with the layer transfer processes for Si thin-film production.[1]

Acknowledgments

The authors thank Professor Fumio Okada for his helpful discussion and comments. This study was partially supported by the Industrial Technology Research Grant Program, 00B64024c, of the New Energy and Industrial Technology Development Organization of Japan, and by the Grant-in-Aid for Scientific Research (A), 15206086, 2003, of the Ministry of Education, Culture, Sports, Science and Technology, Japan.

The University of Tokyo assisted in meeting the publication costs of this article.

List of Symbols

C_{HCl}	HCl concentration, vol %
c_{HCl}	HCl concentration, mol/m^3
c_r	conversion ratio of Si particles
c_{rf}	final conversion ratio in the model
f	ratio of actual surface area of Si particles to that calculated by using the shrinking-core model
f'	ratio of generated area of the activated surface to area of inactive surface lost
k	reaction rate constant, m$^{2.5}$/mol$^{0.5}$/s
M	atomic weight of Si, kg/mol
N	number of active points on each Si particle
P	gas pressure, Pa
Q	total flow rate of reactant gases, sccm
R	gas constant, J/mol/K
R_s	reaction rate of activated Si surfaces, m/s
R_{total}	reaction rate per unit reactor volume, mol/m^3/s
S	outer surface area of Si particles, m^2
S_0	initial surface area of Si particles, m^2
S_a	area of activated surface of Si particles, m^2
S_{all}	overall surface area of reacted Si particles, m^2
S_e	area of etched outer surface of Si particles, m^2
S_V	activated surface area of Si particles per unit reactor volume, m^2/m^3
t(s), t (min)	reaction time
T	temperature, K
V	the volume of the reacted Si particles, m^3
V_0	the volume of the unreacted Si particles, m^3
ρ	density of crystalline Si, kg/m^3

References

1. R. Brendel, *Jpn. J. Appl. Phys., Part 1*, **40**, 4431 (2001).
2. S. Noda, K. Hagiwara, O. Ichikawa, K. Tanabe, T. Yahiro, H. Ohkawa, T. Osawa, and H. Komiyama, in *Proceedings of 29th IEEE Photovoltaic Specialists Conference*, New Orleans, 308 (2002).
3. I. Shiihara and J. Iyoda, *Bull. Chem. Soc. Jpn.*, **32**, 636 (1959).
4. G. A. Lang and T. Stavish, *RCA Rev.*, **24**, 488 (1963).
5. L. V. Gregor, P. Balk, and F. J. Campagna, *IBM J. Res. Dev.*, **9**, 327 (1965).
6. Th. J. M. Kuijer, L. J. Giling, and J. Bloem, *J. Cryst. Growth*, **22**, 29 (1974).
7. P. van der Putte, L. J. Giling, and J. Bloem, *J. Cryst. Growth*, **41**, 133 (1977).
8. J. Bloem and W. A. P. Claassen, *J. Cryst. Growth*, **49**, 435 (1980).
9. C. Dominguez, G. Pastor, and E. Dominguez, *J. Electrochem. Soc.*, **134**, 200 (1987).
10. C. Dominguez, G. Pastor, and E. Dominguez, *J. Electrochem. Soc.*, **134**, 202 (1987).
11. H. Habuka, H. Tsunoda, and T. Otsuka, *J. Electrochem. Soc.*, **145**, 4264 (1998).
12. J. Y. P. Mui, *Corrosion (Houston)*, **41**, 63 (1985).
13. Y. Ohshita and N. Hosoi, *Appl. Phys. Lett.*, **63**, 1216 (1993).
14. S. Bade, U. Hoffmann, and K. Schonert, *Int. J. Min. Process.*, **44-45**, 167 (1996).
15. A. P. Belyi, A. I. Gorbunov, R. M. Flid, S. A. Golubtsov, N. S. Feldshtein, and I. V. Trofimova, *Coll. Czech. Chem. Conn.*, **32**, 1359 (1967).
16. A. P. Belyi, A. I. Gorbunov, R. M. Flid, and S. A. Golubtsov, *Russ. J. Phys. Chem.*, **43**, 637 (1969).
17. K. Subbuag, M. G. Sherman, L. B. Kewis, W. H. Weinberg, J. T. Yates, Jr., and K. C. Janda, *J. Chem. Phys.*, **92**, 5700 (1990).
18. M. L. Wise, B. G. Koehler, P. Gupta, P. A. Coon, and S. M. George, *Surf. Sci.*, **258**, 166 (1991).
19. W. Brenig, H. J. Kreuzer, and S. H. Payne, *Phys. Rev. B*, **67**, 205419 (2003).